REMOTE SENSING INDICATORS OF CHANGES IN ECOSYSTEM FUNCTIONING RELATED TO WILDFIRE DISTURBANCES

Bruno Marcos[1], João Gonçalves[1,2], António Monteiro[1], Domingo Alcaraz-Segura[3], Mário Cunha[2,4], and João Pradinho Honrado[1,2]

1. Research Centre in Biodiversity and Genetic Resources (CIBIO) – Research Network in Biodiversity and Evolutionary Biology Associate Laboratory (InBIO), Porto, Portugal; bruno.marcos@cibio.up.pt
2. Faculty of Sciences of the University of Porto (FCUP), Porto, Portugal
3. Department of Botany, University of Granada, Granada, Spain
4. Geo-Space Sciences Research Centre (CICGE), Porto, Portugal

ABSTRACT

Wildfires cause severe modifications in the matter and energy budgets of ecosystems. Enhanced methods are needed to assess the consequences of those disturbances and the recovery of ecosystems. In this regard, evaluation and monitoring based on ecosystem functioning have advantages over the traditional use of structural features, since functional attributes have shorter time responses to disturbances, and are more directly connected to provision of ecosystem services. Remote sensing allows for quantify ecosystem vulnerability to disturbance as well as spatiotemporal heterogeneity of wildfire disturbance effects on ecosystems.

In this study, we propose and test a framework to assess and monitor changes related to wildfire disturbances, using remotely sensed proxy indicators of critical descriptors of ecosystem functioning (e.g. temperature, albedo, photosynthetic activity, soil moisture), extracted from time-series of MODIS observations. The proposed framework showed an overall accuracy of 98.7% for detection of fire disturbance events, with moderate to good agreement when compared to reference data, while also allowing for simple, fast computation of indicators of fire severity and post-fire recovery. We also discuss the added value of our approach for surveillance of fire occurrence, assessment of fire severity, and monitoring of post-fire recovery.

INTRODUCTION

Worldwide, wildfires are a major threat to a wide range of environmental, social, and economic assets. In Mediterranean Europe – and particularly in Portugal, the country with highest burnt area in the last decade – wildfires have been increasing in number and extension over the last decades, and constitute one of the major ecological disturbances (1). There is thus a need for methods to assess the ecological consequences of those disturbances (2). In this regard, evaluation based on ecosystem functioning (i.e. different aspects of matter and energy fluxes in ecosystems) have advantages over the traditional use of structural features (e.g. species composition or land-cover), since functional attributes have shorter time responses to disturbances (3).

Remote sensing (RS) has particular utility for measuring, monitoring, and developing indicators for fire-related effects on ecosystems. Furthermore, ecosystem functioning can be efficiently monitored through RS, which provides simultaneous estimates of ecosystem function over wide areas (4), in consistent and repeatable measurements, and at the appropriate spatial scales. Continuous (5) or discrete (6) variables can be valuable for the assessment of fire occurrence (7), fire severity (8), and post-fire recovery (1). The land surface temperature (LST) is one of the key parameters in the physics of land-surface processes on regional and global scales, combining the results of all surface–atmosphere interactions and energy fluxes between the atmosphere and the ground; it can be used to discriminate senescent vegetation, monitor drought and estimate surface soil moisture. Furthermore, the tasselled cap transformation (TCT; (9)) features of brightness, greenness, and wetness have been compared to a number of biophysical parameters, including albedo, amount of photosynthetically active vegetation and soil moisture, respectively (10).

Many algorithms have been proposed to detect forest disturbances from remote sensing data (7,11). Two MODIS fire products are available at 1-km resolution: (i) the active fire product detects active fires and other thermal anomalies; and (ii) the burned area product gives the extent of burn scars over a specified time period (12). However, neither of those two products includes estimates of fire severity or post-fire-recovery. Also, the MODIS global disturbance index (MGDI) algorithm is based on annual maximum MODIS LST data and annual maximum MODIS Enhanced Vegetation Index (EVI) data (11,13). The underlying principle is that LST decreases with an increase in vegetation density through latent heat transfer. However, this index can only be calculated at a yearly temporal resolution. Moreover, available products and algorithms generally do not allow for discriminated analysis of multiple attributes of ecosystem functioning.

Since wildfire disturbances cause modifications in the matter and energy budgets of ecosystems (14), an integrative approach capable of evaluating the effects of wildfire disturbance events, integrating the key aspects of matter and energy fluxes (i.e. carbon, water, and energy), is needed for an effective paradigm shift in the monitoring of terrestrial ecosystems. In this study, we aim to improve the assessment of changes in ecosystem functioning due to wildfire disturbance events, using RS-derived indicators of carbon, water, and energy fluxes, in order to: (i) identify individual wildfire disturbance events, in both time and space; (ii) assess the effects of individual wildfire events on ecosystem functioning (i.e. fire severity); and (iii) evaluate the post-fire recovery trajectories (i.e. resilience to single events). Here, we propose a framework to evaluate and monitor changes related to wildfire disturbances, using remotely sensed proxy indicators of important attributes of ecosystem functioning, extracted from MODIS time-series observations.

METHODS

Study area

The study-area corresponds to northern Portugal (Figure 1), a NUTS-II region with an area of approximately 21,265 km^2, which is among the areas with highest incidence of wildfires across Europe (source: EFFIS). Also, it includes a strong climatic gradient (from humid Atlantic to dry Mediterranean) and a large diversity of bedrock, soil types, and land uses.

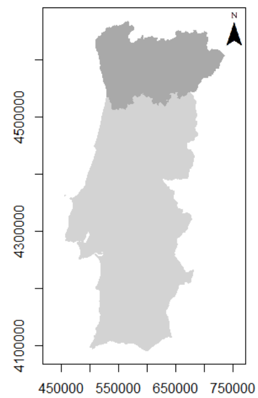

Figure 1: The study-area of northern Portugal (dark grey), within mainland Portugal (light grey).

Data

In this work, we used the MODIS Land Surface Temperature (LST) and Emissivity 8-Day L3 Global 1-km version 5 (MOD11A2), and the MODIS Surface Reflectance 8-Day L3 Global 500m version 5 (MOD09A1) products, for the time period of 2001–2012. These were re-projected to WGS84 / UTM zone 29N, converted to GeoTIFF format, and re-sampled to 500-metres, using MODIS Reprojection Tool (MRT) v4.1 (15). MOD11A2 data are composed from the daily 1-km LST product (MOD11A1) as the average values of clear-sky LSTs during an 8-day period, and includes quality assessment (QA). MOD09A1 provides an estimate of the surface spectral reflectance as it would be measured at ground level in the absence of atmospheric scattering or absorption. Low-level data are corrected for atmospheric gases and aerosols. Each MOD09A1 pixel contains the best possible L2G observation during an 8-day period for bands 1–7 at 500-meter resolution, as well as quality assessment (QA). We used this latter product to compute the MODIS TCT features brightness, greenness, and wetness, following (10) and (16).

As time-series data obtained from high temporal resolution satellite images are hindered by noise arising from atmospheric disturbances, viewing and solar illumination variability, and cloud cover (17), we employed an approach composed of the following three steps, in order to reduce noise in MODIS time-series: (i) using the QA information, we excluded cloud-contaminated values, which were then replaced with the rolling median, with a window size equal to 5; (ii) for blind-rejection of outliers, we used the Hampel identifier (18,19) with a window size equal to 7 – this is regarded as one of the most robust and efficient outlier identifiers, as well as being often considered extremely effective in practice (20) –; and (iii) for smoothing the time-series, Whittaker-Henderson smoother (21,22) with lambda equal to 1 was employed, being able to preserve the characteristics of the time-series, while still reducing noise – this smoother is considered a very attractive alternative to the well-known and popular Savitzky-Golay filter (23), which has several disadvantages (24). All pre-processing steps of MODIS data were undertaken using the package raster (25), within the R statistical programming environment (26).

We also used the Portuguese cartography of burnt areas, which is computed by semi-automated processing of Landsat Thematic Mapper 5 satellite images (27), and is available from the national forest authority (ICNF) in the form of polygons with a minimum mapping area of 5 hectares, for the time period of 1990–2013 (http://www.icnf.pt/portal/florestas/dfci/inc/info-geo). We considered the fire data for the time period of 2001–2012. This data was re-projected to WGS84 / UTM zone 29N and rasterized, using GDAL/OGR v1.11.2 (28), for compatibility with the MODIS data.

Analyses

We used an advanced time-series decomposition technique called STL – Seasonal-Trend decomposition procedure based on the LOcally wEighted regreSsion (LOESS) smoother, which is capable of flexibly decomposing time-series into trend, seasonal and remainder components (29), on MODIS LST and the MODIS TCT features. This decomposition allows for discrimination of both inter- and intra-annual variation within temporal profiles, as well as information of anomalies and remaining noise, in the trend, seasonal, and remainder components, respectively. With this approach, features of general temporal patterns of the pre-fire, fire event, and post-fire periods may be monitored using the trend component, while the seasonal component may be seen as a representation of the "normal" intra-annual variation (due to, e.g. vegetation phenology), to which values of the remainder component can be compared and considered as either anomalies associated with disturbance events (e.g. fires), or noise.

For the detection of the wildfire occurrences, we used an indicator based on the combination of all the four variables considered in this study (i.e. non-decomposed), calculated as: LST/(TCTB+TCTG+TCTW). Similarly to (11,13), the underlying principle is that LST increases with a decrease in vegetation density through latent heat transfer. However, we have also introduced the effects of brightness and wetness, in order to better contrast with the increase in temperature, resulting in larger spike-like patterns, thus allowing for an improved detection and identification of wildfire disturbances. Next, we performed STL decomposition on the z-scores of the ratio between LST and the sum of TCT features (B, G and W), and used the remainder component to determine which values should be considered as potential wildfire disturbances. We then considered as positive detections of wildfire events all values that exceeded 2 standard deviations. Finally, we compared these results with the reference data from the Portuguese fire cartography, using measures of agreement – Sensitivity, Specificity, and Cohen's Kappa (30).

In order to assess fire severity, and evaluate post-fire recovery on vegetation from the identified wildfire disturbance events, the BFAST algorithm, from the R package bfast (7), was used with the TCTG feature. Unlike STL decomposition, BFAST uses an iterative time-series decomposition procedure that allows testing for abrupt changes (i.e. breakpoints) in the time-series, as well as estimating the magnitude of those changes. We then extracted a measure of (relative) fire severity by subtracting the magnitude of the break in the trend component (given by BFAST) of TCTG, to the median of all TCTG values in time-series prior to the fire disturbance event (i.e. pre-fire median). As a measure of post-fire recovery, we used the linear trend component given by BFAST to project the point in time, after the fire event, in which the value of the pre-fire median would be reached. Although post-fire recovery patterns are usually non-linear, the measure we used here provides a fast approximation to an estimate of the rate of post-fire recovery of vegetation.

RESULTS AND DISCUSSION

Ecosystem functional attributes and fire disturbances

Spatial patterns of the median values of the four remotely sensed proxy indicators of ecosystem function are represented in Figure 2. Land surface temperatures (LST) were typically highest on less vegetated or urban areas, while being lowest at mountaintops and closer to water (seen in red and blue/purple, respectively, in Figure 2-A). In the study area, median LST values ranged from approximately 13.9 ºC to 24.9 ºC, in 2001–2012. The lowest median values of tasselled cap brightness (TCTB), a proxy indicator of albedo, were obtained for more densely-vegetated areas (around 0.11), with highest values of 0.55 corresponding to more sparsely-vegetated (seen in red and yellow, respectively, in Figure 2-B). The tasselled cap greenness (TCTG), a vegetation index, had median values ranging from 0.00 to 0.25 (seen in orange to green, respectively, in Figure 2-C), in a gradient from lowest-to-highest amount of photosynthetically active vegetation. Finally, the tasselled cap wetness (TCTW) a remotely sensed proxy indicator of soil moisture, had generally negative median values, ranging from -0.32 in drier areas to -0.04 in wetter areas (e.g. near water; seen in orange to blue, respectively, in Figure 2-D).

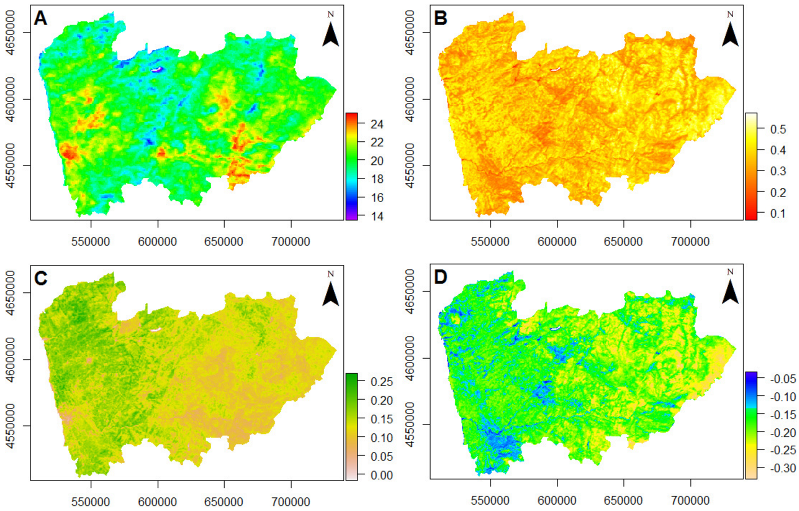

Figure 2: Median values of the indicators of ecosystem functional attributes considered in this study, for the time period 2001–2012, in the study area: (A) Land Surface Temperature (in ºC); (B–D) Tasselled Cap Transformation (TCT) features (unitless) – (B) Brightness (TCTB), (C) Greenness (TCTG), and (D) Wetness (TCTW).

Time-series decomposition of the four variables considered in this study were a useful tool in order to discriminate patterns of disturbance-induced changes, due to wildfire events, from the normal variation (for an example, see Figure 3).

LST usually followed a relatively regular seasonal pattern (Figure 3-A), where winter values ranged from -2.1 ºC to 12.5 ºC, while summer values were between 23.7 ºC and 41.0 ºC. Effects of fire events on this variable were only visible as mild peaks in the non-decomposed time-series, as well as anomalies in the remainder component, and increases in overall LSTs around fire events. TCTB values (Figure 3-B) follow less regular, yet still markedly seasonal, patterns than LST, with winter values ranging from 0.14 to 0.48, while summer values were between 0.27 and 0.61. Although otherwise found in other works (e.g. (31)), obvious breaks (i.e. negative spikes) were typically shown in the STL-remainder component of TCTB, with values of the trend component showing a generalized increase in the post-fire recovery phase. This may be explained by lowered soil brightness due to initial charring, later increasing after this initial phase, while vegetation is still recovering, and the soil brightness increases due to high percentage of exposed soil. The effects of fire disturbances events on TCTG (Figure 3-C) were visibly observable, even in the non-decomposed time-series profiles. Winter TCTG values ranged from 0.03 to 0.21, while summer values were between 0.05 and 0.26. With TCTG seasonality usually following vegetation growth cycles, the trend component typically showed both the impact, as well as the post-fire recovery, associated with wildfire disturbance events. Finally, TCTW (Figure 3-D) also showed a seasonal pattern, although with higher values in winter (between -0.26 and -0.04) and lower values in summer (ranging from -0.37 to -0.11), unlike all other three variables. For TCTW, only the trend component showed typically lowered values after the disturbance events, followed by gradual increase in the post-fire recovery phase.

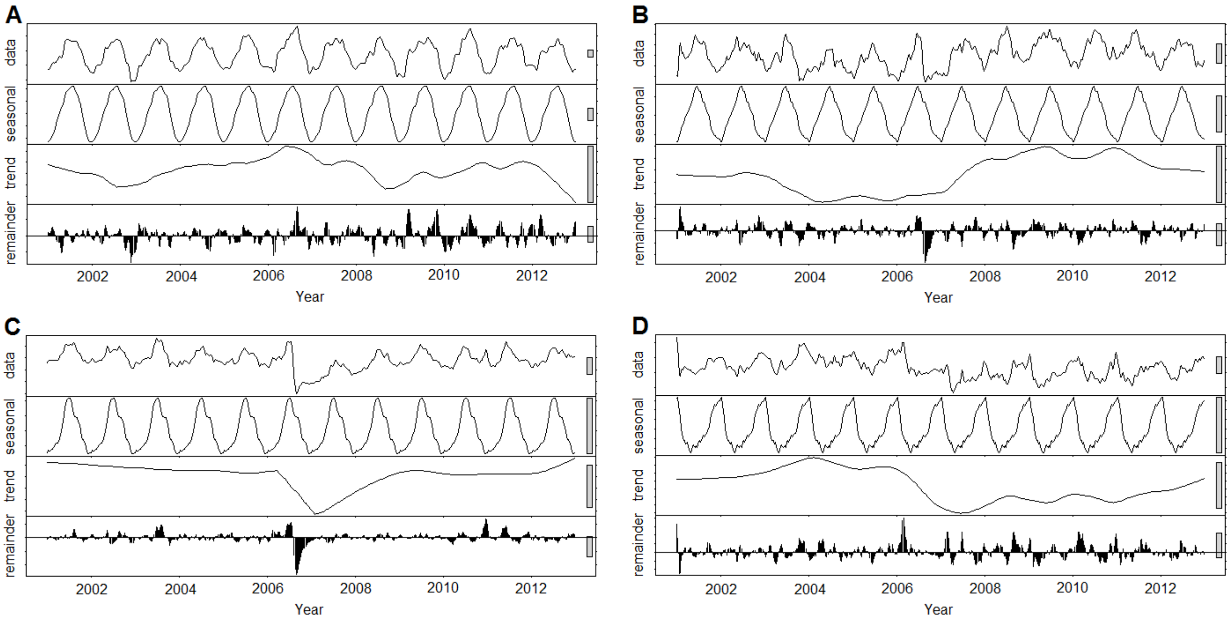

Figure 3: STL decomposition of LST (A), TCTB (B), TCTG (C), and TCTW (D), for an example pixel at approximate coordinates 41º55'47"N 08º18'30"W.

Fire occurrence detection, fire severity, and post-fire recovery

Results from the fire occurrence detection and identification showed moderate to good agreement between the obtained fire occurrences maps and the reference data (see examples in Figure 4), with an overall accuracy of 98.7%, and an overall agreement (as expressed by Cohen's Kappa) of 0.583.

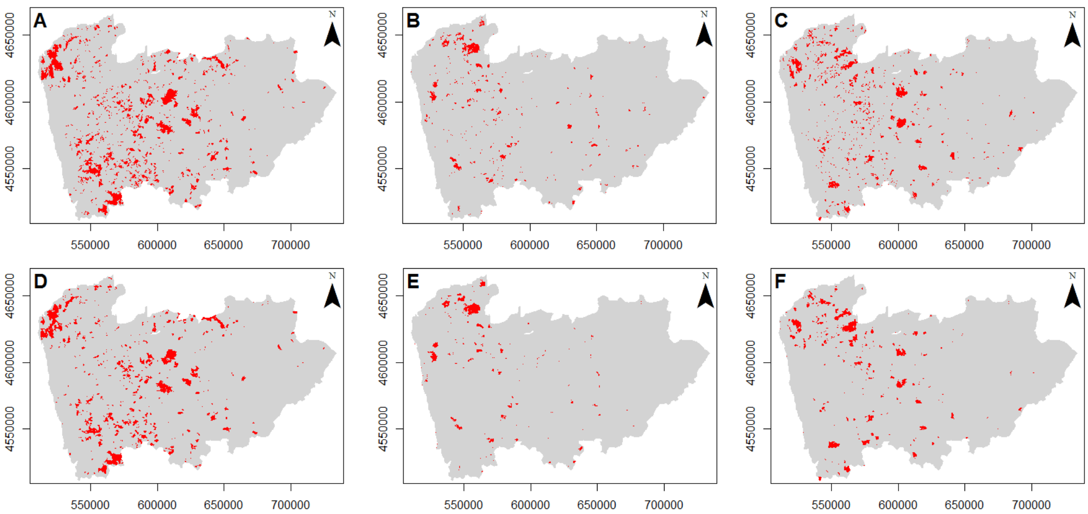

Figure 4: Comparison between reference maps (A–C) of fire occurrences (shown in red), and the ones obtained in this study (D–F), for the years 2005 (A, D), 2006 (B, E), and 2010 (C, F).

True positive rate (also known as Sensitivity) was 57.9%, while true negative rate (or Specificity) was 99.4%, suggesting that a reasonable number of pixels corresponding to fire disturbance events were not successfully detected. In close inspection of map outputs (see examples in Figure 4), we could observe that most of the undetected pixels correspond to two situation types: (i) pixels corresponding to smaller fires; and (ii) pixels in the borders, or in the middle of larger fires. While both situations could be partially explained by the difference in scales inherent to the two data sources (500-metres of MODIS vs. polygons with 5 hectares minimum area based on Landsat data), the latter could also be affected by the fact that, while all burned area was mapped in the reference data regardless of fire severity, fire detection derived from MODIS time-series data could be less sensitive, and thus less effective, wherever fire severity was lower, i.e. when the magnitude of changes in the indicators used were not sufficient to overcome the defined threshold.

Extraction of indicators of fire severity and post-fire recovery from MODIS time-series of observations of TCTG allowed us to add important information about the potential impacts of fire disturbances on ecosystem functioning to the fire occurrence detection. The magnitudes of the breaks in the trend components of TCTG time-series of pixels where a fire was positively detected (illustrated in an example pixel as the blue line in Figure 5) showed a variation in this proxy indicator of fire severity, from 0.004 to 0.198, with a median value of 0.071.

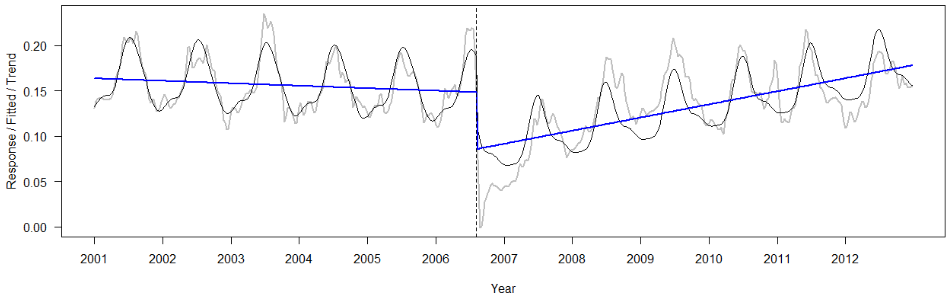

Figure 5: BFAST decomposition of an example pixel at approximate coordinates 41º55'47"N 08º18'30"W. Original data is shown in grey, fitted seasonality is shown in black, and fitted trend is shown in blue.

As for the post-fire recovery, as indicated by the time needed to reach the same value as the pre-fire median TCTG, values ranged from 0.039 years (approximately 14 days) to very large values such as 8751 years, or even infinite (when slopes were negative), meaning that, in some cases, the pre-fire median was never reached within the time period analyses (2001–2012). However, these results are not sufficient to conclude if post-fire recovery of ecosystem functioning did (or will) in fact occur. The median of the values obtained for this indicator was 4.040 years (i.e. approximately 1476 days).

CONCLUSIONS

Time-series of remotely sensed functional variables hold great potential for monitoring changes in important attributes of ecosystem functioning associated with wildfire occurrence as well as during post-fire recovery. Furthermore, we argue that the disturbance indicator used in this work, combining land surface temperatures and tasselled cap features as proxy indicators of ecosystem functional attributes, allows for better discrimination of different aspects of the effects of wildfire disturbances on ecosystem functioning, when compared to other approaches that use only information of, at most, two of those variables (e.g. LST and a vegetation index; (11,13,14)). Our approach for fire occurrence detection, while still holding considerable room for improvement, showed promising performance, at least for burned areas that are big enough for detection using MODIS time-series of observations at 500-metres resolution. Moreover, the approach presented here allows for simple, fast computation of indicators of fire severity and post-fire recovery, providing valuable insights of the effects of wildfire disturbance events on ecosystem functioning to scientists, land managers, and local authorities.

Future research might benefit from data fusion approaches (e.g. STARFM (32)), in order to improve the spatial resolution of input data, consequently improving spatial detail of outputs. Also, new sensors and remote sensing platforms (e.g. Sentinels) offer interesting perspectives for future improvement, provided that long enough time-series can be obtained for monitoring changes in ecosystem functioning.

ACKNOWLEDGEMENTS

This research was financially supported by FEDER funds through the Operational Programme for Competitiveness Factors – COMPETE, and by National Funds through FCT – Foundation for Science and Technology, under the project PTDC/AAG-MAA/4539/2012 / FCOMP-01-0124-FEDER-027863 (IND_CHANGE). João Gonçalves was financially supported by FCT (Portuguese Science Foundation) through PhD grant SFRH/BD/90112/2012.

REFERENCES

1 Bastos A, C M Gouveia, C C DaCamara & R M Trigo, 2011. Modelling post-fire vegetation recovery in Portugal. Biogeosciences, 8(12): 3593-3607.

2 van Leeuwen W J D, G M Casady, D G Neary, S Bautista, J A Alloza, Y Carmel, L Wittenberg, D Malkinson & B J Orr, 2010. Monitoring post-wildfire vegetation response with remotely sensed time-series data in Spain, USA and Israel. International Journal of Wildland Fire, 19(1): p. 75.

3 Alcaraz-Segura D, J Cabello, J M Paruelo & M Delibes, 2008. Trends in the surface vegetation dynamics of the national parks of Spain as observed by satellite sensors. Applied Vegetation Science, 11(4): 431-440.

4 Kerr J T & M Ostrovsky, 2003. From space to species: ecological applications for remote sensing. Trends in Ecology and Evolution, 18(6): 299-305.

5 Coops N C, M A Wulder, D C Duro, T Han & S Berry, 2008. The development of a Canadian dynamic habitat index using multi-temporal satellite estimates of canopy light absorbance. Ecological Indicators, 8(5): 754-766.

6 Alcaraz-Segura D., J Paruelo & J Cabello, 2006. Identification of current ecosystem functional types in the Iberian Peninsula. Global Ecology and Biogeography, 15(2): 200-212.

7 Verbesselt J, R Hyndman, A Zeileis & D Culvenor, 2010. Phenological change detection while accounting for abrupt and gradual trends in satellite image time-series. Remote Sensing of Environment, 114(12): 2970-2980.

8 Veraverbeke S, S Lhermitte, W Verstraeten & R Goossens, 2011. A time-integrated MODIS burn severity assessment using the multi-temporal differenced normalized burn ratio (dNBRMT). International Journal of Applied Earth Observation and Geoinformation, 13: 52-58.

9 Kauth R J & G S Thomas, 1976. The Tasseled Cap – A graphic description of the spectral-temporal development of agricultural crops as seen by Landsat. In: Proceedings of the Symposium on Machine Processing of Remotely Sensed Data (LARS, West Lafayette, Indiana, USA), 41-51.

10 Lobser S E & W B Cohen, 2007. MODIS tasseled cap: land cover characteristics expressed through transformed MODIS data. International Journal of Remote Sensing, 28(22): 5079-5101.

11 Mildrexler D J, M Zhao & S W Running, 2009. Testing a MODIS Global Disturbance Index across North America. Remote Sensing of Environment, 113(10): 2103-2117.

12 Justice C O L Giglio, S Korontzi, J Owens, J T Morisette, D Roy, J Descloitres, S Alleaume, F Petitcolin & Y Kaufman, 2002. The MODIS fire products. Remote Sensing of Environment, 83(1-2): 244-262.

13 Mildrexler D J, M Zhao, F A Heinsch & S W Running, 2007. A new satellite-based methodology for continental-scale disturbance detection. Ecological Applications, 17(1): 235-250.

14 Petropoulos G, T N Carlson, M J Wooster & S Islam, 2009. A review of Ts/VI remote sensing based methods for the retrieval of land surface energy fluxes and soil surface moisture. Progress in Physical Geography, 33 (2): 224-250.

15 DAAC, 2006. MODIS Reprojection Tool User's Manual, 57 pp.

16 Zhang X, C B Schaaf, M A Friedl, A H Strahler, F Gao & J C F Hodges, 2002. MODIS tasseled cap transformation and its utility. In: Geoscience and Remote Sensing Symposium (IEEE International), 2: 1063-1065.

17 Hird J N & G J McDermid, 2009. Noise reduction of NDVI time-series: An empirical comparison of selected techniques. Remote Sensing of Environment, 113(1): 248-258.

18 Hampel F R, 1971. A General Qualitative Definition of Robustness. The Annals of Mathematical Statistics, 42(6): 1887-1896.

19 Hampel F R, 1974. The Influence Curve and its Role in Robust Estimation. Journal of the American Statistical Association, 69(346): 383-393.

20 Pearson, 2002. Outliers in process modeling and identification. Control Systems Technology, 10(1): 55-63.

21 Whittaker E T, 1923. On a new method of graduation. Proceedings of the Edinburgh Mathematical Society, 41: 63-75.

22 Henderson R, 1924. A new method of graduation. Transactions of the Actuarial Society of America, 25: 29-40.

23 Savitzky A & M J E Golay, 1964. Smoothing and differentiation of data by simplified least squares procedures. Analytical Chemistry, 36: 1627-1639.

24 Eilers P H C, 2003. A perfect smoother. Analytical Chemistry, 75: 3631-3636.

25 Hijmans R J, 2015. raster: Geographic Data Analysis and Modeling. R package version 2.3-40. URL http://CRAN.R-project.org/package=raster.

26 R Core Team, 2015. R: A language and environment for statistical computing. Version 3.2. R Foundation for Statistical Computing, Vienna, Austria. URL http://www.R-project.org/.

27 Moreira F, P Vaz, F Catry & J Silva, 2009. Regional variations in wildfire susceptibility of land-cover types in Portugal: Implications for landscape management to minimize fire hazard. International Journal of Wildland Fire, 18: 563-574.

28 GDAL, 2015. GDAL – Geospatial Data Abstraction Library: Version 1.11.2. Open Source Geospatial Foundation. URL http://gdal.osgeo.org.

29 Cleveland R B, W S Cleveland, J E McRae & I Terpening, 1990. STL: A Seasonal-Trend decomposition procedure based on Loess. Journal of Official Statistics, 6(1): 3-73.

30 Cohen J, 1960. A coefficient of agreement for nominal scales. Educational and Psychological Measurement, 20(1): 37-46.

31 Hilker T, M A Wulder, N C Coops, J Linke, G McDermid, J G Masek, F Gao & J G White, 2009. A new data fusion model for high spatial- and temporal-resolution mapping of forest disturbance based on Landsat and MODIS. Remote Sensing of Environment, 113(8): 1613-1627.

32 Gao F, M D Jessup, J Masek, M Schwaller & F Hall, 2006. On the blending of the Landsat and MODIS surface reflectance: predicting daily Landsat surface reflectance. IEEE Transactions on Geoscience and Remote Sensing, 44(8): 2207-2218.